

Supplementary Information

Integration of Inverse Nanocone Array based Bismuth Vanadate Photoanodes and Bandgap-Tunable Perovskite Solar Cells for Efficient Self-Powered Solar Water Splitting

Shuang Xiao,^{a,b,c†} Chen Hu,^{a,†} He Lin,^a Xiangyue Meng,^a Yang Bai,^a Teng Zhang,^a Yinglong Yang,^a Yongquan Qu,^c Keyou Yan,^d Jianbin Xu,^d Yongcai Qiu,^{a,d,e,*} Shihe Yang^{a,b*}

^aDepartment of Chemistry, The Hong Kong University of Science and Technology, Clear Water Bay, Kowloon, Hong Kong, China

^bGuangdong Key Lab of Nano-Micro Material Research, School of Chemical Biology and Biotechnology, Shenzhen Graduate School, Peking University, Shenzhen, China.

^cJoint School of Sustainable Development and Frontier Institute of Science and Technology, Xi'an Jiaotong University, Yan Xiang Road, Xi'an, China

^dDepartment of Electronic Engineering, The Chinese University of Hong Kong, Shatin, New Territories, Hong Kong, China

^fCollege of Environment and Energy, South China University of Technology, Guangzhou, China

*CORRESPONDING AUTHOR E-mail: (chqiuyc@gmail.com; chsyang@ust.hk)

† These authors contribute equally to this work.

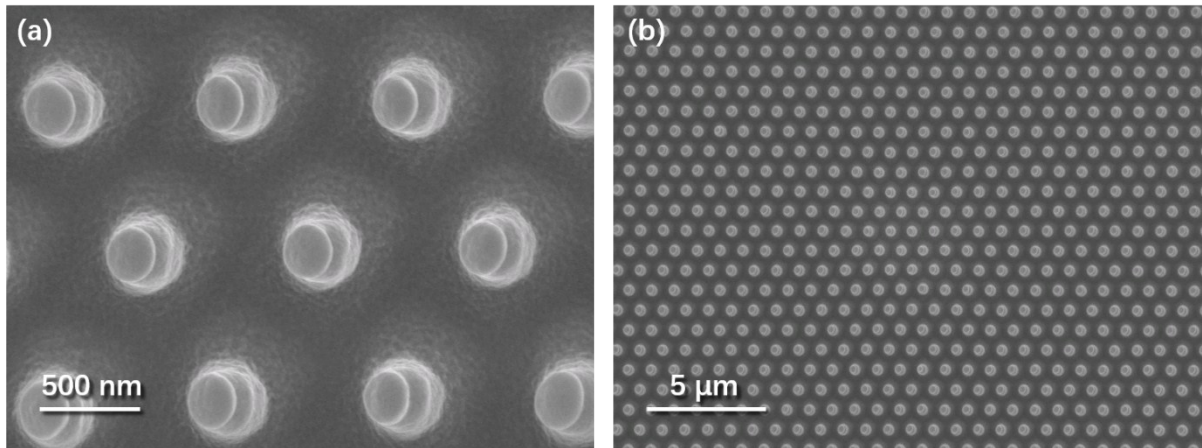


Fig. S1. SEM images of PDMS mold. (a) High magnified image shows the pitch has a cone-like shape. (b) Low magnified image shows that the nanocone array on PDMS mold is highly ordered in a large scale.

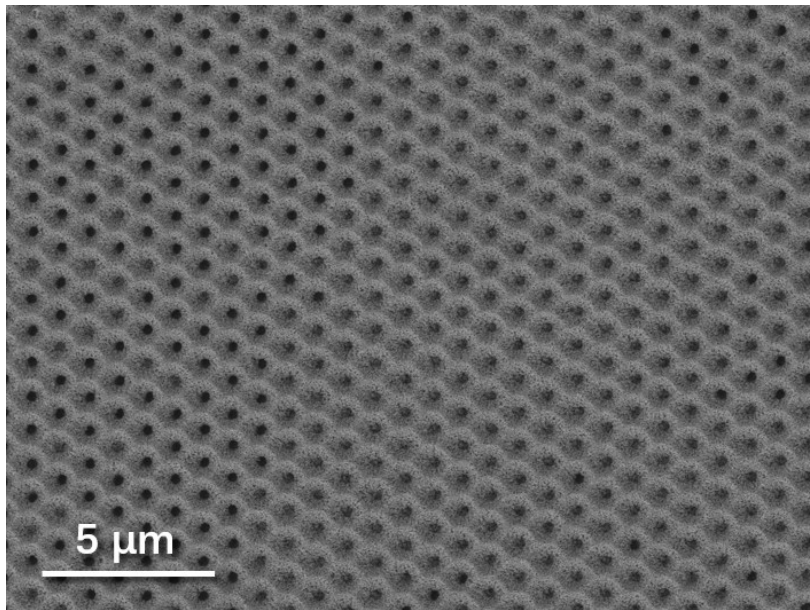


Fig. S2. SEM image of 3D ICA-TiO₂, showing that the ICA structure is highly ordered in a large scale.

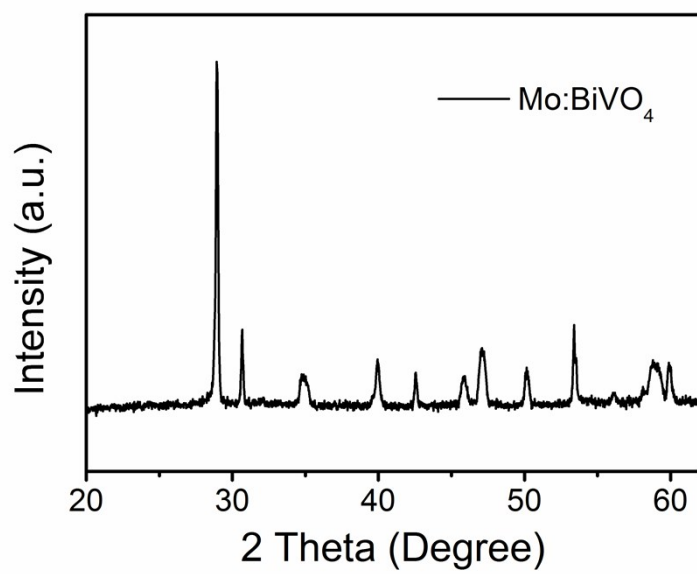


Fig. S3. The XRD pattern of the Mo:BiVO₄ deposited by the sol-gel method.

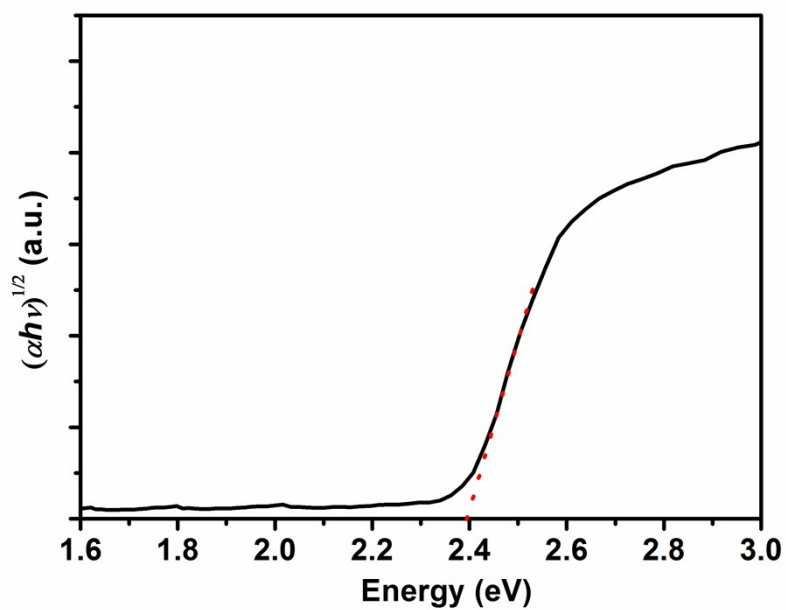


Fig. S4. The absorption curve of monolithic Mo:BiVO₄ of $(\alpha h\nu)^{1/2}$ versus photon energy ($h\nu$). The estimated bandgap is around 2.4 eV.

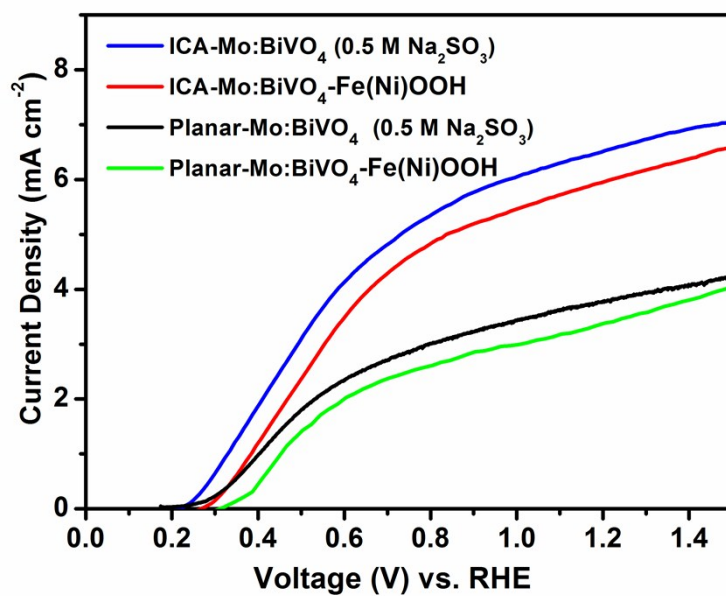


Fig. S5. J - V curves of the ICA-Mo:BiVO₄ in KPH buffer solution with hole scavenger (blue line), the ICA-Mo:BiVO₄-Fe(Ni)OOH in KPH buffer solution (red line), the planar-Mo:BiVO₄ in KPH buffer solution with hole scavenger (black line) and the planar-Mo:BiVO₄-Fe(Ni)OOH in KPH buffer solution (green line).

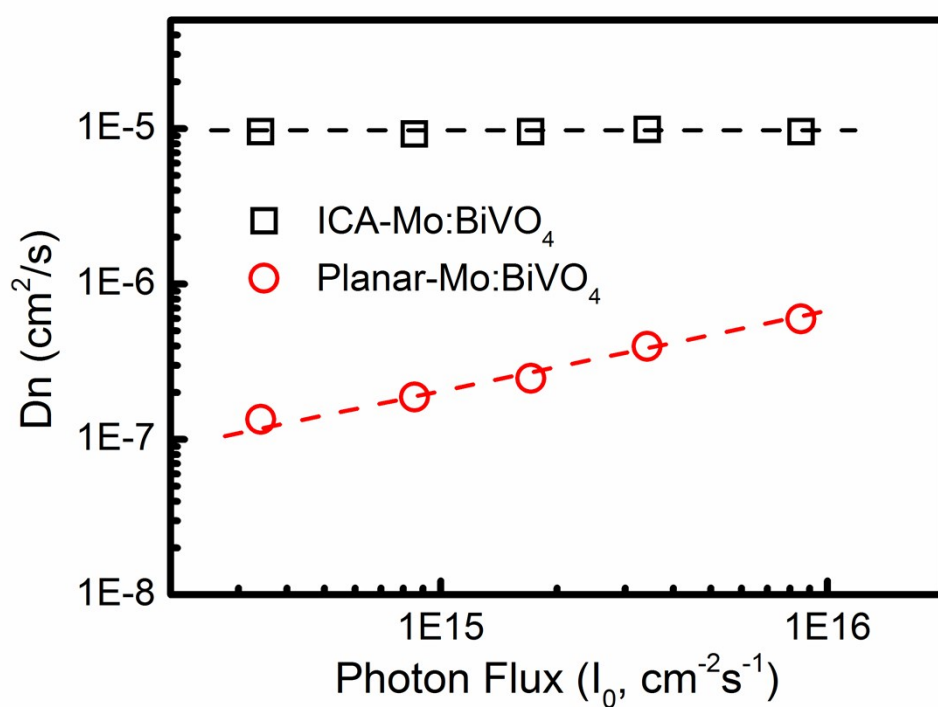


Fig. S6. Intensity modulated photocurrent spectroscopy (IMPS) tests for the ICA-Mo:BiVO₄ in KPH buffer solution with hole scavenger (black dashed line) and the planar-Mo:BiVO₄ in KPH buffer solution with hole scavenger (red dashed line).

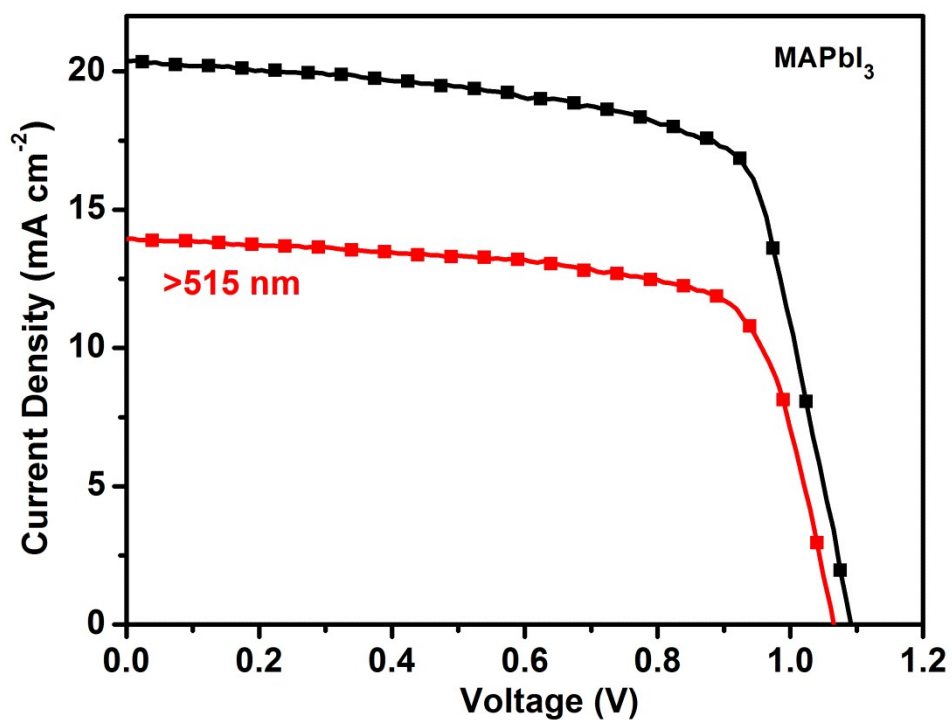


Fig. S7. J - V curves of the NiO-based inverted MAPbI₃ PSCs. Black: tested in the entire wavelength region at 1 Sun; Red: tested in the wavelength region of >515 nm. The V_{oc} has a 25 mV deduction from 1.090 to 1.065 V and J_{sc} varies from 20.3 mA cm⁻² to 14.0 mA cm⁻².

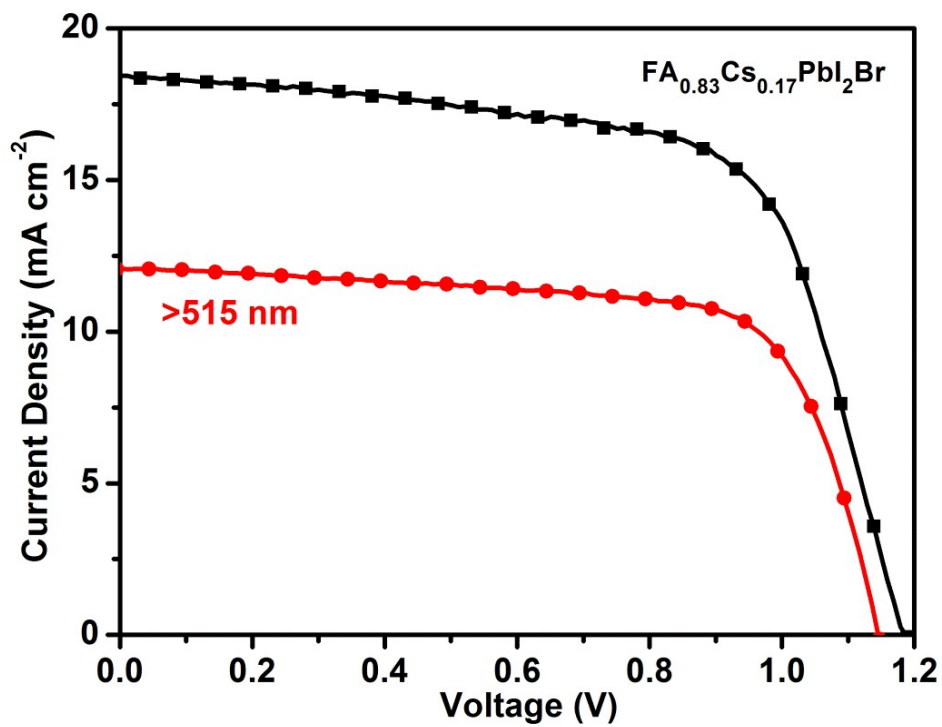


Fig. S8. J - V curves of the NiO-based inverted $\text{FA}_{0.83}\text{Cs}_{0.17}\text{PbI}_2\text{Br}$ PSCs. Black: tested in the entire wavelength region at 1 Sun; Red: tested in the wavelength region of >515 nm. The V_{oc} has a 39 mV deduction from 1.184 to 1.145 V and J_{sc} varies from 18.4 mA cm^{-2} to 12.1 mA cm^{-2} .

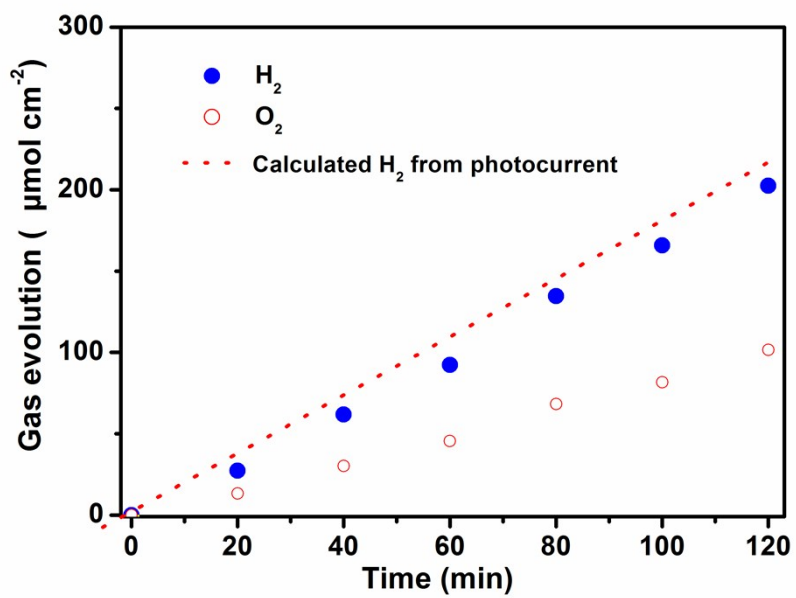


Fig. S9. H₂ and O₂ production from the tandem device and its theoretical gas production rate of the tandem device.